Melt Rheological Properties of Polypropylene/SEBS (Styrene–Ethylene Butylene–Styrene Block Copolymer) Blends

A. K. GUPTA and S. N. PURWAR, *Centre for Materials Science and Technology, Indian Institute of Technology, New Delhi-110 016, India*

Synopsis

Study of melt rheological properties of the blends of polypropylene (PP) with styrene–ethylene butylene–styrene block copolymer (SEBS), at blending ratios 5–20% SEBS, is reported. Results illustrate the effects of (i) blend composition and (ii) shear rate or shear stress on melt viscosity and melt elasticity and the extrudate distortion. In general, blending of PP with SEBS results in a decrease of its melt viscosity, processing temperatures, and the tendency of extrudate distortion. However, the properties depend on blending ratio. A blending ratio around 5–10% SEBS seems optimum from the point of view of desirable improvement in processability behavior.

INTRODUCTION

Use of elastomers as the impact modifiers of polymers is well documented in the literature.[1] Blending of polymers with elastomers produces not only improvement in the impact properties but also gives suitable combination of other physical and mechanical properties of the blend. Such polymer/elastomer blends may have the disadvantages, characteristic of the immiscible blends, such as lower strength and modulus, and the advantages of better processability and flexural and impact properties suitable for various applications.

Blends of polypropylene (PP) with various impact modifiers have been investigated in the literature, as, for example, ethylene propylene rubber,[1–3] hydrogenated polybutadiene,[4] styrene butadiene rubber,[5] acrylonitrile butadiene styrene terepolymer,[6] etc. A recent addition to the family of thermoplastic elastomers is the triblock copolymer styrene–ethylene butylene–styrene (SEBS), which is obtained by hydrogenation of the butadiene sequence of styrene–butadiene–styrene triblock copolymer (SBS).[7,8]

It is known[8,9] that the blends of SEBS with thermoplastic polyolefins have the advantage of higher service temperature and solvent resistance than most thermoplastic polyolefin blends with dienes. Studies on mechanical properties of the blends of SEBS with high density polyethylene (HDPE) and polystyrene (PS) are reported recently by Lindsey, Paul, and Barlow.[7] Another study involving SEBS is reported by Siegfried, Thomas, and Sperling,[10] which describes the rheology and morphology of thermoplastic interpenetrating polymer networks (IPN) developed with SEBS and styrene, methacrylic acid, and isoprene monomers.

In this paper we present a study of the melt rheological and impact properties of PP/SEBS blends, prepared by solution blending technique. Melt rheology

Journal of Applied Polymer Science. Vol. 29, 1079–1093 (1984)
© 1984 John Wiley & Sons, Inc. CCC 0021-8995/84/041079-15$04.00

data, obtained on a piston type capillary rheometer, are used to obtain shear stress vs. shear rate relationship, melt viscosity, and melt elasticity parameters of this blend at various blend compositions. Effect of blending on melt fracture behavior of PP is illustrated by extrudate distortion. Scanning electron microscopic measurements on cryogenically fractured ends of the extrudates are reported to illustrate the state of dispersion of the SEBS phase in these blends.

EXPERIMENTAL

Materials. PP used in this work was Koylene S-1730 (melt flow index 1.7) supplied by Indian Petrochemicals Corporation, Ltd. The SEBS triblock copolymer used was Kraton G-1652 supplied by Shell Chemical Co. It has polystyrene end blocks which comprise 30% of the mass and a hydrogenated polybutadiene midblock, which is equivalent to ethylene–butylene 1 copolymer (EB). Approximate block molecular weights are[10]: 8×10^3 g/mol, S; 39×10^3 g/mol, EB; 8×10^3 g/mol, S.

Preparation of Blends. Blends of PP with SEBS, with blend compositions 5, 10, 15, and 20 wt % SEBS, were prepared by solution-blending technique. Solution of PP in xylene was mixed with solution of SEBS in the same solvent, both at 80°C, with constant stirring. Blends were recovered by precipitation with methanol and then washed with methanol. These were then dried first at ambient temperature and thereafter in a vacuum oven.

The blends obtained from solution blending were not subject to any subsequent mechanical mixing; hence the dispersion of the two phases in these samples would be characteristic of that obtained on coprecipitation.

Measurements. Melt flow properties were measured on a piston type capillary rheometer (Koka Flow Tester of Shimadzu Seisakusho, Ltd.), using circular die ($L/R = 10$) flat at the entrance region. Measurements were made at pressures in the range of 10–110 kg/cm^2. Other details about the experimental procedure and the analysis of the data are provided at relevant places in subsequent discussion.

Izod impact strength of the notched samples was measured at room temperature, using ASTM D-628 specifications, on the samples cut from compression moulded sheets of 2 mm thickness. A minimum of five samples were tested for each blend composition, and the deviation was less than 8% from the mean value in all cases.

Scanning electron micrographs of the cryogenically fractured ends of the extrudate were recorded on a Stereoscan S4-10 of Cambridge Scientific Instruments, Ltd. Samples were etched with xylene at room temperature for 30 min to dissolve away the SEBS component.

RESULTS AND DISCUSSION

In these capillary rheometer measurements, both the standard procedures[11] were followed, viz., (i) temperature elevation method and (ii) fixed temperature method. Results of temperature elevation method are presented as the variations in the "plasticity curve" of PP on blending with SEBS. The fixed temperature data were recorded as the "flow curves" from which various parameters of flow were calculated at three temperatures 180°C, 190°C, and 200°C.

Plasticity Curves. Plasticity curves, which represent temperature dependence of the piston (or plunger) displacement at constant pressure, for PP, SEBS, and the PP/SEBS blends of varying blend composition are shown in Figure 1. These curves are reproduced as obtained on the recorder chart. It should be noted that the y-axis (i.e., plunger displacement) scale is identical in all the cases, while the x-axis (i.e., the temperature) differed from sample to sample as marked on each individual curve. Owing to the constant speed of the recorder drum, the x-axis is a linear function of time. Sample amount and the rate of power supplied to the heater were kept constant in all the cases and the temperature of the sample was recorded through a thermocouple in contact with the sample close to the die region. Hence these data not only indicate the different rates of increase of temperature in different samples, but also show the time dependency of viscous flow. Some differences in heat capacities of these different samples might be expected due to their differing compositions. The time dependency in viscous flow is known[12] for certain pseudoplastic and dilatant fluids. From these plasticity curves it is apparent that the time dependency of the flow varies gradually with varying blend composition from the extreme cases of one individual component (i.e., PP) to the other (i.e., SEBS) of the blend.

Plasticity curve of PP shows several distinct regions as indicated by points A, B, C, D, and E on Figure 1(a). Region AB of downward movement of the plunger is associated with compaction of the polymer chips in the temperature region close to the softening point (T_s).[11] The region BD, which is the melting

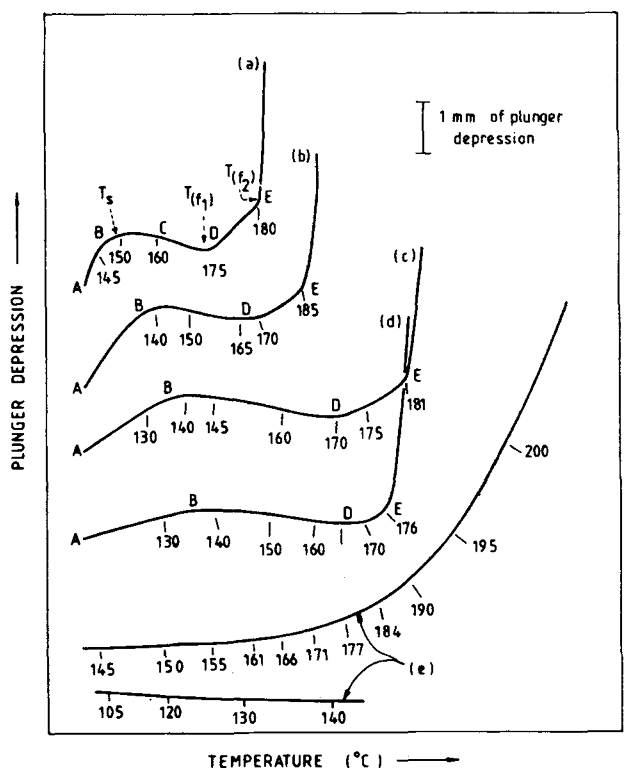

Fig. 1. Plasticity curves of PP, SEBS, and their blends obtained at pressure 30 kg/cm^2 and die L/R = 4: (a) PP; (b) PP/SEBS 5%; (c) PP/SEBS 10%; (d) PP/SEBS 20%; (e) SEBS.

region, represents an upward movement of the plunger due to the melt elasticity and/or volume expansion on melting of the polymer. The midpoint C of this melting region coincides with melting temperature T_m of the PP. The flow through the die orifice starts beyond point D, where the continuous downward movement of the plunger sets in. The flow region on the curve shows two distinct parts. The region DE represents slower rate of flow, while in the region beyond E the flow is faster and insignificantly dependent on temperature. The curve for SEBS [Fig. 1(e)], on the other hand, does not show distinct regions like the case of PP. Slight upward movement of plunger in the region 105–140°C is seen, and the flow commenced at 150°C, with the rate of flow increasing gradually with increasing temperature. The slower rate of flow of SEBS than PP is apparently due to higher melt viscosity of SEBS.

In PP/SEBS blends, the increasing SEBS content produces the following changes in the plasticity curve of PP:

(1) The region AB becomes less steep, and the temperature corresponding to point B (i.e., T_s) gradually decreases.

(2) The region BDE flattens and the flow rate in the region DE decreases. The temperature corresponding to the midpoint C of the region BCD also decreases, implying a slight decrease of T_m. The flow temperatures T_{f_1} and T_{f_2} corresponding to the beginning of the two flow regions, i.e., points D and E, respectively, also decrease.

Values of the temperatures at points B, C, D, and E, i.e., T_s, T_{f_1} and T_{f_2} respectively are shown in Table I for these samples. Decrease of about 10–15°C in all these temperatures is apparent over the studied range of blend composition.

Shear Stress—Shear Rate Curves. Data at constant temperatures and varying pressures were used to evaluate the shear stress and shear rate relationships in these samples. Shear stress at the wall, $(\tau_w)_{app}$, was calculated using the following expression[13] neglecting the end correction term for these data at constant L/R ratio of the die:

$$(\tau_w)_{app} = \Delta P/2\,(L/R) \tag{1}$$

where ΔP is the pressure difference between the entrance and exit of the capillary. The shear rate $\dot{\gamma}$ was determined according to the expression[13]

$$\dot{\gamma} = 4Q/\pi R^3 \tag{2}$$

where Q is the volumetric flow rate and R is the radius of the capillary. The apparent melt viscosity η_{app} was evaluated as

$$\eta_{app} = (\tau_w)_{app}/\dot{\gamma} \tag{3}$$

TABLE I
Values of T_s, T_{f_1} and T_{f_2} for the Various Samples

Sample	T_s (°C)	T_{f_1} (°C)	T_{f_2} (°C)
PP	150	175	180
PP/SEBS 5%	142	167	185
PP/SEBS 10%	140	170	181
PP/SEBS 20%	140	169	176
SEBS	—	150	—

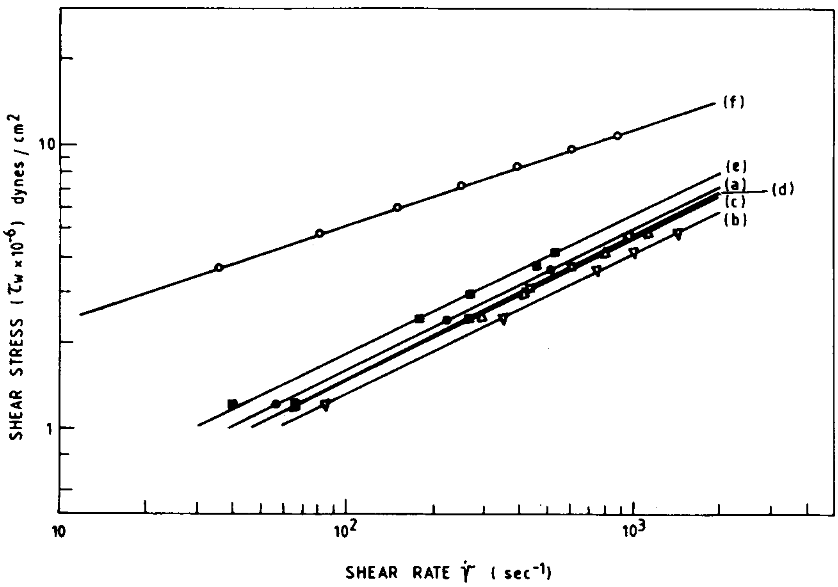

Fig. 2. Shear stress–shear rate curves at 200°C of: (a) PP (b) PP/SEBS 5%; (c) PP/SEBS 10%; (d) PP/SEBS 15% (e) PP/SEBS 20%; (f) SEBS.

Variations of shear stress vs. shear rate were quite linear over the entire range studied, confirming the validity of the power-law relationship for these samples. The shear stress–shear rate curves for these various samples at a given temperature 200°C are shown in Figure 2 as a typical example of these data. Values of the exponent, n, of the power law relation[13]

$$(\tau_w)_{\text{app}} = K\dot{\gamma}^n \tag{4}$$

determined from these data for the various samples are shown in Table II. Values of n lower than unity clearly support the pseudoplastic behavior of the melt for all these samples, and the insignificant variation of n indicates that the pseudoplasticity changes inappreciably with blend composition.

Melt Viscosity. Variation of apparent melt viscosity (η_{app}) with shear stress $(\tau_w)_{\text{app}}$ at the three temperatures of measurement are shown in Figures 3 and 4 for these various samples. At any given temperature η_{app} decreases with increasing shear stress, showing linear variations on the log–log scale. Slopes of

TABLE II
Values of Power Law Exponent (n) According to Eq. (4) and Activation Energy for Viscous Flow (ΔE) for the Various Samples

Sample	n At 180°C	n At 190°C	n At 200°C	ΔE (kcal/mol)
PP	0.46	0.47	0.50	11.8
PP/SEBS (5%)	0.51	0.47	0.49	14.1
PP/SEBS (10%)	0.50	0.49	0.49	15.5
PP/SEBS (15%)	—	—	0.57	—
PP/SEBS (20%)	0.47	0.47	0.49	15.4
SEBS	0.31	0.31	0.34	23.5

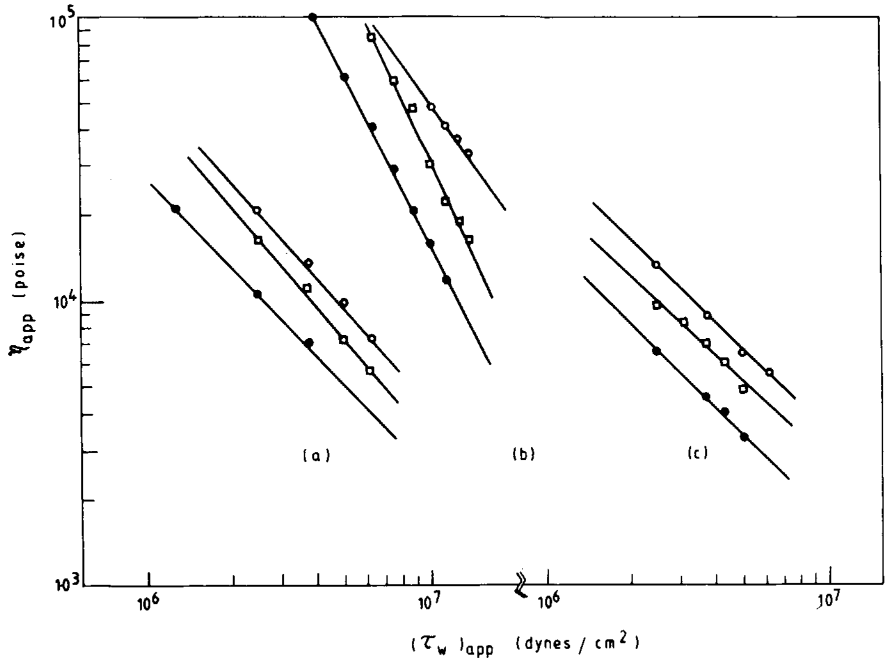

Fig. 3. Variation of apparent melt viscosity (η_{app}) with shear stress for (a) PP, (b) SEBS, and (c) PP/SEBS 5%, at three temperatures (°C): (○) 180; (□) 190; (●) 200.

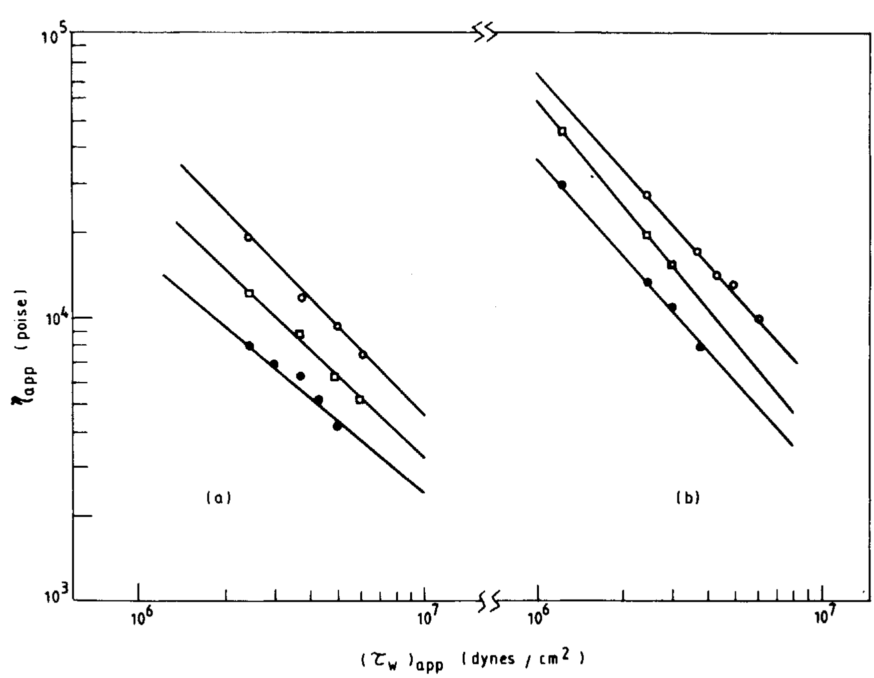

Fig. 4. Variation of apparent melt viscosity (η_{app}) with shear stress for (a) PP/SEBS 10% and (b) PP/SEBS 20% at three temperatures (°C): (○) 180; (□) 190; (●) 200.

these curves are quite consistent with the power-law relation[13] for the pseudoplastic fluids obeying eq. (4):

$$\eta_{\text{app}} = K^{1/n} \, (\tau_w)_{\text{app}}^{(n-1)/n} \tag{5}$$

with values of n consistent with those shown in Table II.

Temperature dependence of melt viscosity is represented in Figure 5 as the Arrhenius plots, log η_{app} vs. $1/T$. Activation energies (ΔE) calculated from the slopes of these plots are shown in Table II. Activation energy for the viscous flow of the melt increases with increasing SEBS content of the blend.

Variation of melt viscosity with blend composition is shown in Figure 6 at the three constant temperatures. Minima in melt viscosity are found around the 5% SEBS content in these blends. Up to about 15% SEBS content, the melt viscosity of the blend remains less than that of PP, while at 20% SEBS content it becomes higher than that of PP. It may be recalled that the melt viscosity of SEBS is higher than that of the PP used in this study.

Melt Elasticity. Parameters characterising melt elasticity, such as die–swell ratio, first normal stress difference, recoverable shear strain, and the apparent shear modulus, were evaluated from these data. The die–swell ratio is D_i/D, where D_i and D are the diameters of the extrudate and the die, respectively. The first normal stress difference $(\tau_{11} - \tau_{22})$ is calculated according to the Tanner's equation[14]

$$\tau_{11} - \tau_{22} = 2(\tau_w)_{\text{app}} \, [2(D_i/D)^6 - 2]^{1/2} \tag{6}$$

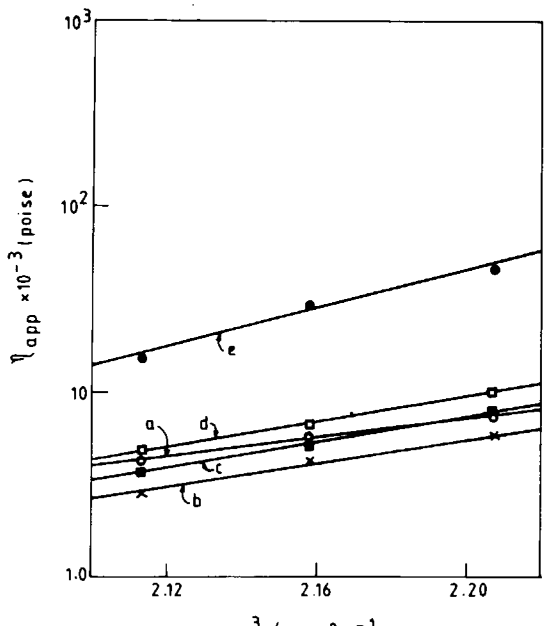

Fig. 5. Arrhenius plots, log η_{app} vs. $1/T$, of the melt viscosity data for PP/SEBS blends at constant shear stress $[(\tau_w)_{\text{app}} = 6 \times 10^6 \text{ dyn/cm}^2]$: (a) PP; (b) PP/SEBS 5%; (c) PP/SEBS 10%; (d) PP/SEBS 20%; (e) SEBS.

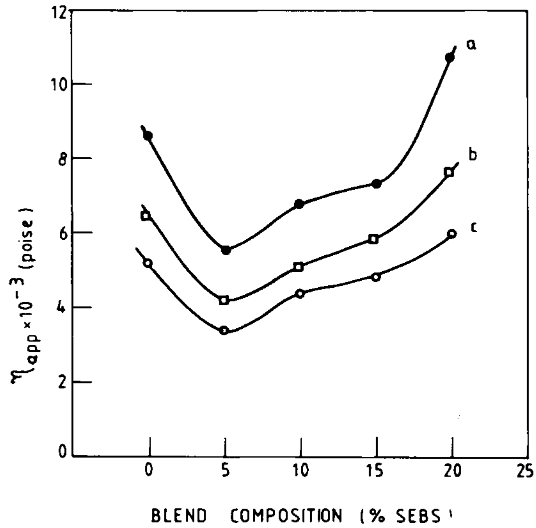

Fig. 6. Variation of apparent melt viscosity (η_{app}) with blend composition for PP/SEBS blends at 200°C at constant shear stress (dyn/cm²): (a) 3×10^6; (b) 4×10^6; (c) 5×10^6.

Recoverable shear strain (γ_R) and the apparent shear modulus (G) were calculated from the following relations[13,15]

$$\gamma_R = (\tau_{11} - \tau_{22})/2(\tau_w)_{app} \tag{7}$$

$$G = (\tau_w)_{app}/\gamma_R \tag{8}$$

Values of these elasticity parameters at several shear stresses are shown in Table III for the various samples. Variations of these melt elasticity parameters

TABLE III
Values of the Melt Elasticity Parameters for the PP/SEBS Blends at Various Shear Stresses

Sample	$(\tau_w)_{app} \times 10^{-6}$ (dyn/cm²)	D_i/D	$(\tau_{11} - \tau_{22}) \times 10^{-7}$ (dyn/cm²)	γ_R	$G \times 10^{-5}$ (dyn/cm²)
PP	1.47	2.06	9.03	12.28	2.99
	1.96	2.24	15.52	15.83	3.09
	2.45	2.50	27.03	22.05	2.78
	2.94	2.80	45.62	31.00	2.37
PP/SEBS 5%	1.47	1.92	7.28	9.91	3.71
	1.96	2.16	13.91	14.18	3.46
	2.45	2.46	25.75	21.00	2.92
	2.94	2.70	26.90	27.80	2.65
PP/SEBS 10%	1.47	1.72	5.19	7.05	5.21
	1.96	1.87	8.96	9.14	5.36
	2.45	2.21	18.63	15.20	4.03
	2.94	2.35	26.92	18.30	4.02
PP/SEBS 15%	1.47	1.62	4.73	6.43	5.72
	1.96	1.76	7.43	7.58	6.47
	2.45	1.98	13.35	10.88	5.63
	2.94	2.17	21.16	14.38	5.11
P/SEBS 20%	1.47	1.65	4.55	6.19	5.94
	1.96	1.72	6.92	7.05	6.95
	2.45	1.90	11.76	9.60	6.38
	2.94	2.03	17.28	11.75	6.29

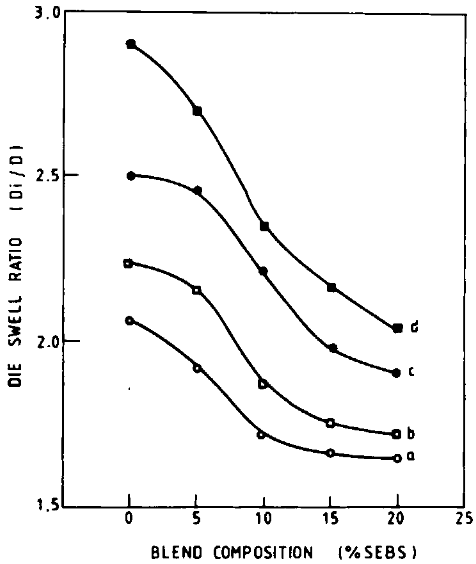

Fig. 7. Variation of die–swell ratio with blend composition at constant shear stress (dyn/cm^2): 9a) 1.47 × 10^6; (b) 1.96 × 10^6; (c) 2.45 × 10^6; (d) 2.94 × 10^6.

with blend composition and shear stress or shear rate are presented in Figures 7, 8, and 9 as two types of representation. Variations of (D_i/D) and $(\tau_{11} - \tau_{22})$ are shown as functions of blend composition at several constant shear stresses (Figs. 7 and 8), while those of G and γ_R are presented as functions of shear rate [similar to the conventional representation used by other authors[15] at various constant blend compositions (Fig. 9)].

A sigmoidal shape of the variation of these melt elasticity parameters with

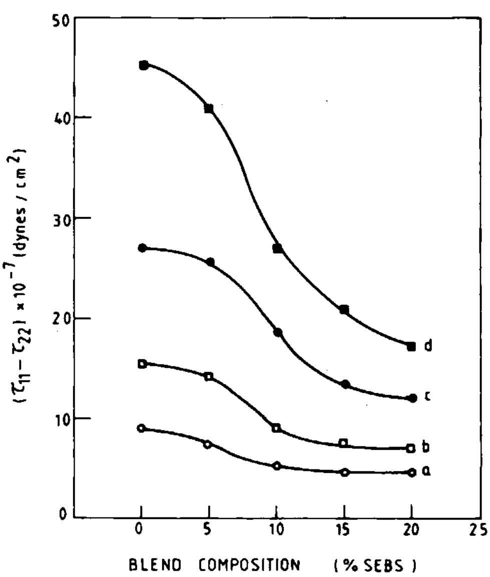

Fig. 8. Variation of first normal stress difference $(\tau_{11} - \tau_{22})$ with blend composition at constant shear stress (dyn/cm^2): (a) 1.47 × 10^6; (b) 1.96 × 10^6; (c) 2.45 × 10^6; (d) 2.94 × 10^6.

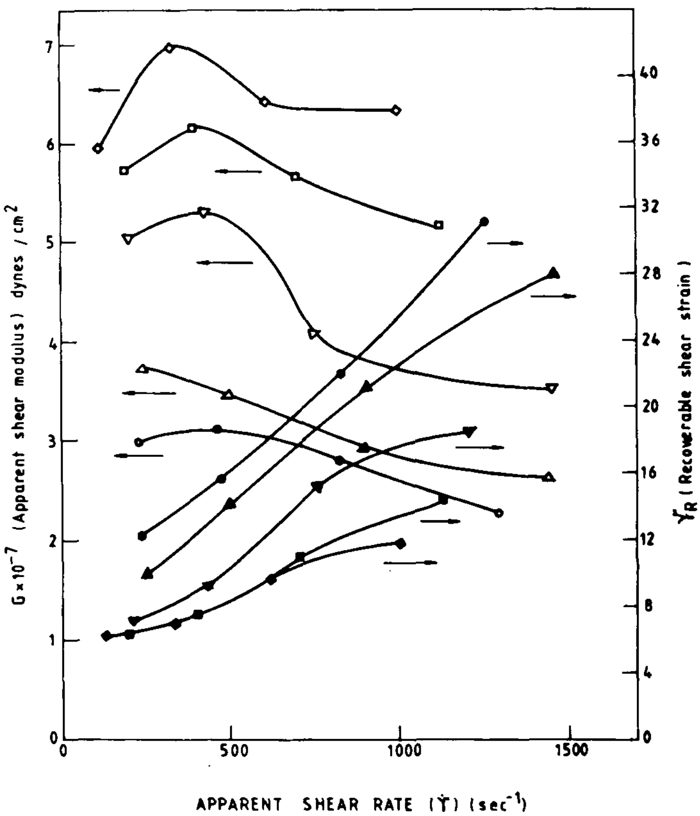

Fig. 9. Variation of recoverable shear strain (γ_R) and apparent shear modulus (G) as function of shear rate at various constant blend compositions (SEBS/PP): (●,○) 0/100; (▲,△) 5195; (▼,▽) 10/90; (■,□) 15/85; (◆,◇) 20/80.

blend composition was obtained in all cases, as shown, for example, in Figures 7 and 8 for the die–swell ratio and the first normal stress difference. At any given shear stress, the decrease in melt elasticity with increasing SEBS content of the blend was slower in the regions 0–5% and above 15% SEBS content. The total decrease, for example, of the die–swell ratio was by a factor of 1.25–1.45 in the studied range of blend composition, depending on the shear stress. Recoverable shear strain (γ_R) increases, and the apparent shear modulus (G) decreases with increasing shear rate. At any constant shear rate, γ_R decreases and G increases with increasing SEBS content of the blend, and the sigmoidal shapes of these variations, with the aforesaid characteristics, were observed.

Extrudate Distortion. Melt fracture behavior of PP, which gives rise to distortion of the extrudate surface at high shear stress, is considerably affected by blending PP with SEBS. Photographs of the extrudates are presented in Figure 10 as the typical examples of the observed effect of blend composition and shear stress on the distortion of extrudate surface of these blends.

At constant shear stress, i.e., the case represented by Figure 10(a), the tendency of extrudate distortion decreases in the following order: PP > blend with 5% SEBS > blend with 10% SEBS. However, the blends with 15% and 20% SEBS showed almost no distortion of extrudate [Fig. 10(a)].

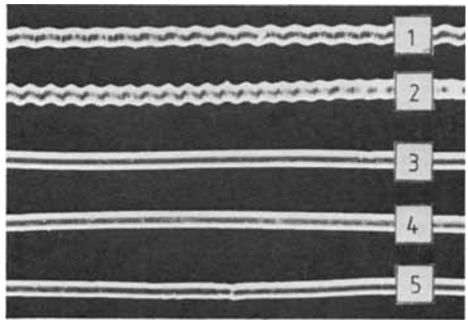

(a)

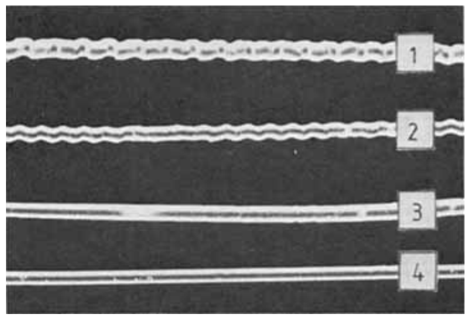

(b)

Fig. 10. Distortions of extrudate surface: (a) At constant shear stress 1.47×10^6 dyn/cm^2: (1) PP; (2) PP/SEBS (5%); (3) PP/SEBS (10%); (4) PP/SEBS (15%) (5) PP/SEBS (20%); (b) at constant blend composition (5% SEBS) and different shear stress (dyn/cm^2): (1) 2.96×10^6; (2) 2.45×10^6; (3) 1.96×10^6; (4) 1.47×10^6.

For any given composition, extrudate distortion was found to occur only when the shear stress exceeded a certain critical value, and thereafter it increased with increasing shear stress. The critical shear stress $(\tau_w)^*_{\mathrm{app}}$, above which the extrudate distortion starts appearing in these blends, increased with increasing SEBS content of the blend.

These effects of blend composition and shear stress on the extrudate distortion are quite consistent with the melt elasticity behavior of these samples. A reduction in melt elasticity would decrease the melt fracture or the extrudate distortion. Occurrence of extrudate distortion or melt fracture has been explained in terms of the recoverable shear strain.[13] For a given material, the elastic strain energy that can be held in the shear field has got a limit and, when this limit is crossed, the extra amount of elastic strain energy may be converted into surface free energy, resulting in the distortion of the extrudate. As shown in the previous section, blending with SEBS decreases the recoverable shear strain, which is consistent with the observed behavior of extrudate distortion of these samples.

Impact Strength. Variation of impact strength of these blends with blend composition is shown in Figure 11. It is seen that the impact strength increases with increasing SEBS content. At low SEBS content (less than 10%) the increase of impact strength is quite marginal, whereas above 15% SEBS content the impact strength increased rapidly with increasing elastomer content. Furthermore, the samples with 20% SEBS content did not break during the impact testing, presumably owing to their high elastomer content.

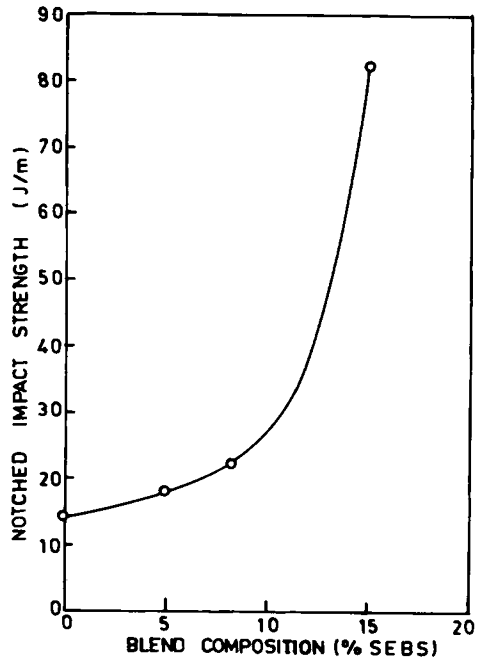

Fig. 11. Variation of impact strength with blend composition of the compression molded samples of PP/SEBS blends.

Lower impact strength at low SEBS content could be due to the smaller size of the SEBS domains. The effect of small size domains of SEBS was observed on the melt viscosity of the blend in the region of low SEBS content, where the melt viscosity decreased (see Fig. 6) due to the plasticization effect of the small domains of the discrete phase.

These data show a sixfold increase in impact strength of PP on blending it with 15 wt % SEBS by solution-blending technique. Further improvements in impact strength might be possible by improving the dispersion of the two phases of the blend by mechanical mixing of the coprecipitated blends.

State of Dispersion. Scanning electron micrographs of cryogenically fractured surfaces of the extrudates of these blends extruded at two shear stresses $(\tau_w)_{app} = 1.47 \times 10^6$ and 1.96×10^6 dyn/cm^2 are shown in Figures 11 and 12 respectively. The fracture surfaces were etched with xylene for 30 min at room temperature to remove the discrete phase SEBS. These micrographs show the occurrence of sufficiently localized nonspherical (or irregularly shaped) domains of discrete phase in these blends. In addition to these large size domains, there are also some narrow elongated regions which are apparently formed by elongation of small droplets (or domains) of the discrete phase along the lines of flow. Blends with high SEBS content, 15–20% SEBS, show larger localized domains of the discrete phase.

Lower tendency of deformation of the larger sized domains of SEBS is also apparent from these micrographs, whereas the smaller domains are well elongated into threadlike shapes. In the case of blends with higher SEBS contents there would be greater number of large-size domains of the discrete phase than in the

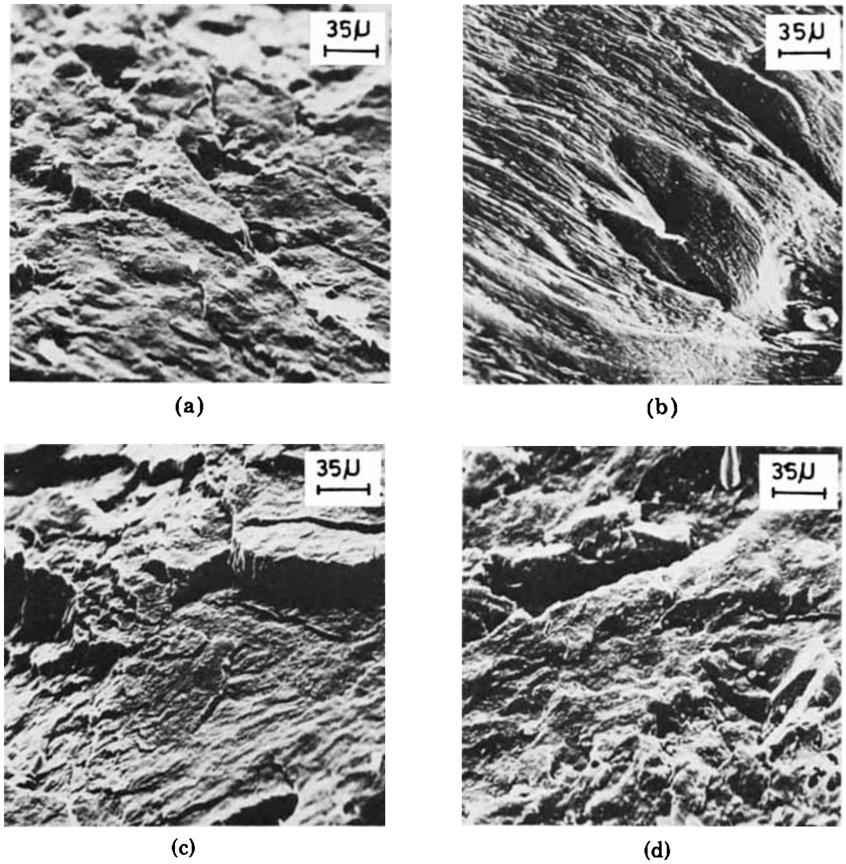

Fig. 12. Scanning electron micrographs of fractured ends of extrudates obtained at shear stress 1.47×10^6 dyn/cm^2: (a) PP/SEBS (5%); (b) PP/SEBS (10%); (c) PP/SEBS (15%); (d) PP/SEBS (20%).

case of blends with 5–10% SEBS content. These big-size domains might be the cause of greater obstruction to flow, which might account for the observed high melt viscosity in the cases of blends with 15–20% SEBS content. At lower SEBS content (5–10%), the decrease of melt viscosity seems an effect of plasticization produced by smaller size domains which are apprently elongated and aligned along the flow line and thereby ease the flow.

These blends show a characteristic behavior that the melt viscosity goes through a minimum at around 5–10% SEBS content and then again increases at higher SEBS content, while the melt elasticity decreases sigmoidally with increasing SEBS content. Lower melt elasticity of the blends with high SEBS content might be due to either one or both the following effects:

(i) lower deformability of the discrete phase domains,

(ii) possibility of slippage at the interphase boundaries, which may account for discontinuities in both shear rate and shear stress.

Deformability of viscoelastic domains is related to the capacity of storing recoverable elastic energy. Elasticity of melt, for example, the recoverable shear strain (γ_R), is lower for the blends with high SEBS content, which is consistent with the lower deformability of the large SEBS domains in the blends revealed by scanning electron micrographs.

Since the mixing of these blends is done in solution, the domain formation and internal structure of the domains of SEBS would be governed by not only the mutual affinity of PS and EB blocks but also on the relative affinity of EB and PS blocks with PP. The two polymers, PP and SEBS, would have some time to segregate on precipitation. Small amounts of SEBS might form small particles which acted as plasticizer of SEBS which are dragged along during the melt flow.

Solubility parameters evaluated[10] for EB and PS blocks are 7.90 and 9.07 $(cal/cc)^{1/2}$, respectively, which seem to suggest some segregation of EB and PS in the SEBS domains. In such a situation, either EB or PS may form a mixed phase depending on their relative affinity with PP. Incompatibility of PP and PS is well known in the literature,[13] whereas the affinity of PP with EB is not certain. If, on the basis of the known[7] affinity of EB with another polyolefin HDPE, one believes in the affinity of EB with PP, then the flowing matrix in these blends might be viewed as the mixed PP and EB phase in which PS do-

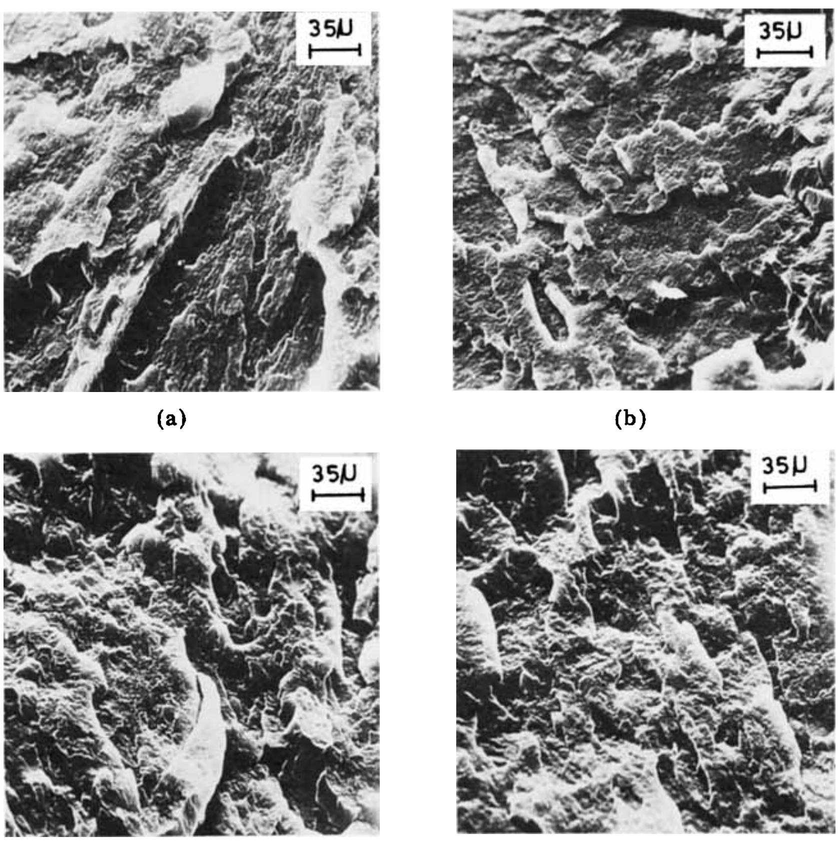

(c) (d)

Fig. 13. Scanning electron micrographs of fractured ends of extrudates obtained at shear stress 1.96×10^6 dyn/cm^2: (a) PP/SEBS (5%); (b) PP/SEBS (10%); (c) PP/SEBS (15%); (d) PP/SEBS (20%).

mains are being dragged along. Experimental values of solubility parameters reported by other authors[16–18] for PP [9.2 $(cal/cc)^{1/2}$] and PS [8.5–9.1 $(cal/cc)^{1/2}$] seem to further provoke the doubt about the formation of mixed EB and PP phase.

However, these scanning electron micrographs (Figs. 12 and 13) seem to support that the discrete phase domains that are dragged along with the flowing matrix are constituted of SEBS as a whole and not PS alone. The voids left after dissolving away the SEBS on etching is characteristic of the shapes of the domains during the flow with sufficiently sharp domain boundaries. There is apparently no trace of dissolved out EB phase at the domain boundaries.

CONCLUSIONS

Blending of PP with SEBS decreases the softening and flow temperatures. The power law relationship between shear stress and shear strain is obeyed over the entire range of shear stress studied and all the blend compositions, with power law exponent varying from 0.3 to 0.5, suggesting pseudoplastic nature of the melt. Melt viscosity decreased to a minimum at about 5% SEBS content. Melt viscosity of the blend is lower than PP only up to 15% SEBS content; at still higher SEBS content (20%), the melt viscosity of the blend is higher than PP. Melt elasticity decreases with increasing SEBS content, the decrease being more steep in the region of 5–15% SEBS content.

Extrudate distortion (or melt fracture) of PP decreases on blending with SEBS. Impact strength increases with increasing SEBS content; blending with 15% SEBS produces a sixfold increase in impact strength of PP. Scanning electron microscopy reveals the formation of discrete SEBS domains dispersed in PP matrix. Smaller domains have greater tendency to deform during the flow than the bigger domains.

References

1. D. R. Paul and S. Newman, *Polymer Blends* Academic, New York (1978), Vol. 2.
2. M. Kakugo and H. Sadanori, *Sumitomo Kagaku Tokushugo*, 1, 22 (1979).
3. F. C. Stehling, T. Huff, C. S. Speed, and G. Wissler, *J. Appl. Polym. Sci.*, **26**, 2693 (1981).
4. A. F. Halasa, D. W. Carlson, and J. E. Hall, U.S. Pat. 4, 226, 952 (1980).
5. G. G. A. Bohn, G. R. Hamed, and L. E. Yescelius, Ger. Offen. 2, 825, 697 (1978).
6. C. Markin and H. L. William, *J. Appl. Polym. Sci.*, **25**, 2451 (1980).
7. C. R. Lindsey, D. R. Paul, and J. W. Barlow, *J. Appl. Polym. Sci.*, **26**, 1 (1981).
8. P. Dreyfuss, L. J. Fetters, and D. R. Hansen, *Rubber Chem. Technol.*, **53**, 728 (1980).
9. W. R. Hendricks, W. R. Haefle, and F. T. Bishop, U.S. Pat. 3, 639, 163 (1972).
10. D. L. Siegfried, D. A. Thomas, and L. H. Sperling, *J. Appl. Polym. Sci.*, **26**, 177 (1981).
11. T. Arai, *A Guide to Testing of Rheological Properties by Koka Flow Tester*, Maruzen Co., Tokyo, 1958.
12. R. S. Lenk, *Polymer Rheology* Applied Science, London, 1978, p. 15.
13. C. D. Han, *Rheology in Polymer Processing*, Academic, New York, 1976.
14. R. I. Tanner, *J. Polym. Sci.*, *A-2*, **8**, 2067 (1970).
15. A. F. Plochocki, in *Polymer Blends* D. R. Paul and S. Newman, Eds., Academic, New York, 1978, Vol. 2.
16. J. F. Voeks, *J. Polym. Sci. Part A*, **2**, 5319 (1964).
17. R. A. Hayes, *J. Appl. Polym. Sci.*, **5**, 318 (1961).
18. G. M. Bristow and W. F. Watson, *Trans. Faraday Soc.*, **54**, 1742 (1958).

Received May 17, 1983
Accepted August 1, 1983